Accepted Manuscript

Hybrid chemistry: part 4. Discovery of etravirine–VRX-480773 hybrids as potent HIV-1 non-nucleoside reverse transcriptase inhibitors

Zheng-Yong Wan, Yuan Tao, Ya-Feng Wang, Tian-Qi Mao, Hong Yin, Fen-Er Chen, Hu-Ri Piao, Erik De Clercq, Dirk Daelemans, Christophe Pannecouque

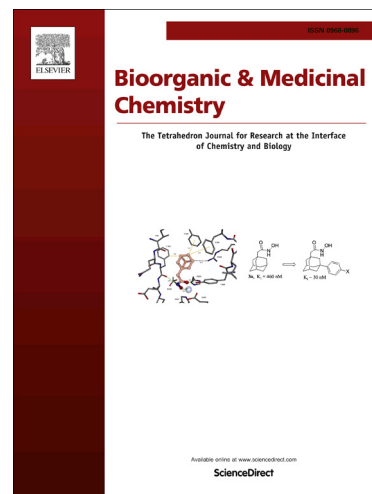Please cite this article as: Wan, Z-Y., Tao, Y., Wang, Y-F., Mao, T-Q., Yin, H., Chen, F-E., Piao, H-R., Clercq, E.D., Daelemans, D., Pannecouque, C., Hybrid chemistry: part 4. Discovery of etravirine–VRX-480773 hybrids as potent HIV-1 non-nucleoside reverse transcriptase inhibitors, *Bioorganic & Medicinal Chemistry* (2015), doi: http://dx.doi.org/10.1016/j.bmc.2015.06.048

Graphical Abstract

Hybrid chemistry: part 4. Discovery of etravirine–VRX-480773 hybrids as potent HIV-1 non-nucleoside reverse transcriptase inhibitors

Leave this area blank for abstract info.

Zheng-Yong Wan[a], Yuan Tao[a], Ya-Feng Wang[a], Tian-Qi Mao[a,b], Hong Yin[a], Fen-Er Chen[a,b], Hu-Ri Piao[c], Erik De Clercq[d], Dirk Daelemans[d], Christophe Pannecouque[d]

[a]Department of Chemistry, Fudan University, Shanghai 200433, People's Republic of China
[b]Institute of Biomedical Science, Fudan University, Shanghai 200433, People's Republic of China
[c] Key Laboratory of Natural Resources and Functional Molecules of the Changbai Mountain, Affiliated Ministry of Education, Yanbian University, Yanji 133000, People's Republic of China
[d]Rega Institute for Medical Research, Katholieke Universiteit Leuven, 10 Minderbroedersstraat, B-3000 Leuven, Belgium

Hybrid chemistry: part 4. Discovery of etravirine–VRX-480773 hybrids as potent HIV-1 non-nucleoside reverse transcriptase inhibitors
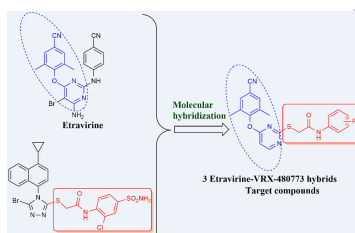
Zheng-Yong Wan[a], Yuan Tao[a], Ya-Feng Wang[a], Tian-Qi Mao[a,b], Hong Yin[a], Fen-Er Chen[a,b,*], Hu-Ri Piao[c,*], Erik De Clercq[d], Dirk Daelemans[d], Christophe Pannecouque[d]

[a]Department of Chemistry, Fudan University, Shanghai 200433, People's Republic of China

[b]Institute of Biomedical Science, Fudan University, Shanghai 200433, People's Republic of China

[c]Key Laboratory of Natural Resources and Functional Molecules of the Changbai Mountain, Affiliated Ministry of Education, Yanbian University, Yanji 133000, People's Republic of China

[d]Rega Institute for Medical Research, Katholieke Universiteit Leuven, 10 Minderbroedersstraat, B-3000 Leuven, Belgium

ARTICLE INFO

ABSTRACT

A novel series of etravirine–VRX-480773 hybrids were designed using structure-guided molecular hybridization strategy and fusing the pharmacophore templates of etravirine and VRX-480773. The anti-HIV-1 activity and cytotoxicty was evaluated in MT-4 cell cultures. The most active hybrid compound in this series, *N*-(2-chlorophenyl)-2-((4-(4-cyano-2,6-dimethylphenoxy)pyrimidin-2-yl)thio)acetamide **3d** (EC_{50} = 0.24 μM, SI > 1225), was more potent than delavirdine (EC_{50} = 0.66 μM, SI > 67) in the anti-HIV-1 *in vitro* cellular assay. Studies of structure-activity relationships established a correlation between anti-HIV activity and the substitution pattern of the acetanilide group.

1. Introduction

The discovery of etravirine **1** (TMC125, Fig. 1) is a comprehensive result of the coordinated multidisciplinary endeavor lasting for more than 20 years of research on non-nucleoside reverse transcriptase inhibitors (NNRTIs).[1] This promising NNRTI was approved by the FDA in 2008 for AIDS therapy owing to potency against both wild-type (WT) and mutant virus strains. Another clinical candidate NNRTI, VRX-480773 **2**[2] (Fig. 1) originated from high-throughput screening (HTS) of compound libraries as a second generation NNRTI, showed resilience to most NNRTI-resistant clinical HIV-1 isolates. However, there is still a great need for additional new chemical entities with improved affinity and efficacy profiles and higher genetic barriers to resistance.
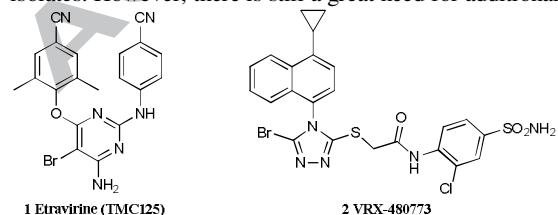
Figure 1. Structures of etravirine and VRX-480773.
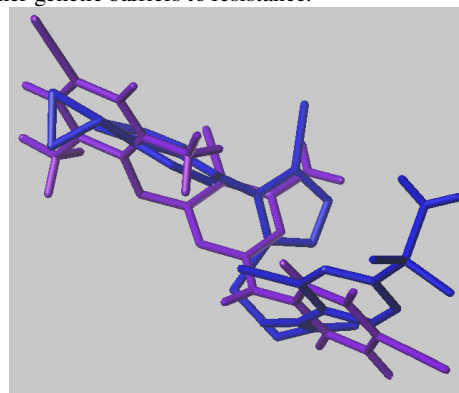
Figure 2. Superposition of lower-energy docking binding conformations of etravirine (purple) and VRX-480773 (blue) in the binding pocket of HIV-1 RT (protein removed for clarity).

The present work is an extension of our ongoing efforts towards developing effective NNRTIs through a hybrid pharmacophore approach[3-5], and one that uses etravirine and

---

∗ Corresponding author. Tel.: +86 21 65643809; fax: +86 21 65643811; e-mail: rfchen@fudan.edu.cn

∗ Corresponding author. Tel.: +86 43 3243003; fax: +86 43 32435004; e-mail: piaohuri@aliyun.com
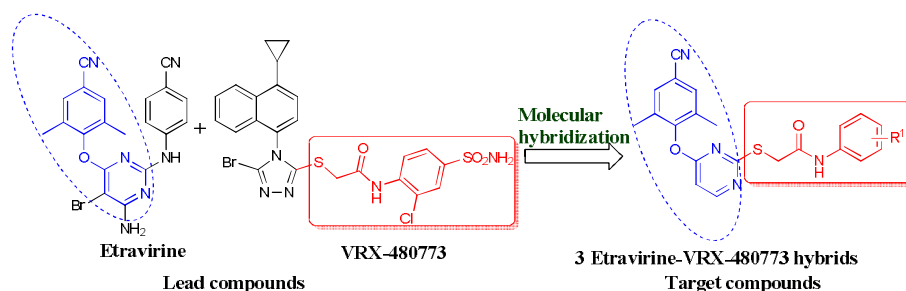
Figure 3. Design of etravirine–VRX-480773 hybrids **3** based on structure-guided molecular hybridization.

Scheme 1. Synthetic route of target compounds **3a-u**. Reagents and conditions: (a) 4-hydroxy-3,5-dimethylbenzonitrile, NaH, THF, 40 $^{\circ}$C, 6 h; (b) thiourea, EtOH, reflux, 4.5 h; (c) substituted α-bromoacetamide **7a-u**, KOt-Bu, DMF, r.t., 1 h.

Table 1
Biological activities of compounds **3a-u** in MT-4 cells[a]

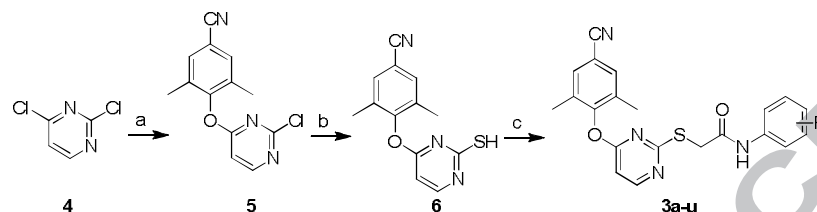| Compds	R	EC$_{50}$[b] (µM)			CC$_{50}$[c] (µM)	SI[d]	pKa[e]	Log P[e]	MR[e] (cm^3)	PSA[f] (Å^2)
		III$_B$	K103N+Y181C	HIV-2						
3a	H	>320	>320	>320	>320	1	0.6±0.8	5.62±0.52	108.36±0.4	87.91
3b	3-F	8.1±0.5	>306	>306	>306	>38	0.6±0.9	6.15±0.59	108.47±0.4	87.91
3c	4-F	8.0±2.4	>306	>306	>306	>38	0.6±0.8	6.01±0.57	108.47±0.4	87.91
3d	2-Cl	0.24±0.05	≥10.9	>294	>294	>1225	0.5±0.9	5.82±0.54	113.19±0.4	87.91
3e	3-Cl	8.0±2.3	>294	>294	>294	>37	0.6±0.9	6.34±0.54	113.19±0.4	87.91
3f	4-Cl	3.9±1.9	>294	>294	>294	>75	0.6±0.9	6.59±0.54	113.19±0.4	87.91
3g	2,4-DiCl	1.2±0.6	>272	>272	>272	>227	0.5±0.9	6.80±0.55	118.01±0.4	87.91
3h	3,4-DiCl	5.3±1.4	>89	>89	89±7	17	0.6±0.9	7.18±0.56	118.01±0.4	87.91
3i	3,5-DiCl	10.8±2.8	>41	>41	≥41	>3.7	0.5±0.9	7.08±0.56	118.01±0.4	87.91
3j	4-Br	1.4±0.3	>24	>24	24±3.7	17	0.6±0.9	6.83±0.57	116.08±0.4	87.91
3k	2-NO$_2$	0.34±0.04	>287	>287	>287	>844	0.4±0.9	5.54±0.54	114.39±0.4	133.73
3l	3-NO$_2$	41±7	>287	>287	>287	>7	0.5±0.9	6.01±0.54	114.39±0.4	133.73
3m	4-NO$_2$	1.4±0.3	>287	>287	>287	>205	0.6±0.9	6.20±0.55	114.39±0.4	133.73
3n	4-CN	4.3±0.7	>301	>301	>301	>70	0.6±0.9	5.90±0.58	112.93±0.4	111.70
3o	2-F-4-CN	6.0±1.3	>288	>288	>288	>48	0.5±0.9	5.48±0.71	113.04±0.4	111.70
3p	4-SO$_2$NH$_2$	7.9±1.9	>266	>266	>266	>34	0.6±0.9	4.54±0.57	120.80±0.4	148.07
3q	2-Me	5.9±1.7	>309	>309	>309	>52	0.6±0.8	6.08±0.52	112.98±0.4	87.91
3r	4-Me	5.1±1.0	>309	>309	>309	>61	0.6±0.8	6.08±0.52	112.98±0.4	87.91
3s	2-Me-4-SO$_2$NH$_2$	0.81±0.19	>46	>46	46±12	57	0.6±0.9	5.00±0.57	125.42±0.4	148.07
3t	4-MeO	7.3±1.3	>69	>69	≥69	≥9	0.8±0.7	5.63±0.53	114.72±0.4	97.14
3u	4-OH	8.3±1.3	>71	>71	71±17	9	0.9±0.6	4.87±0.53	109.89±0.4	108.14
DEV		0.66±0.61	>44	ND[g]	>44	>67	----	----	124.34±0.4	110.43
ETV		0.0041±0.0002	0.025±0.002	ND[g]	>4.6	>1122	<3[9]	>5[9]	106.87±0.4	120.65
VRX-480773		0.00014±0.000032[2]	0.00023±0.000025[2]	ND[g]	5.82[10]	41571	1.7±0.8	6.81±1.01	141.40±0.5	119.98

[a] All data represent mean values for at least three separate experiments.
[b] EC$_{50}$: effective concentration required to protect the cell against viral cytopathicity by 50% in MT-4 cells.
[c] CC$_{50}$: cytotoxic concentration of compound that reduces the normal uninfected MT-4 cell viability by 50%.
[d] SI: selectivity index, ratio CC$_{50}$/EC$_{50}$ (WT).
[e] Predicted by using software ACD.
[f] Predicted by using software ChemAxon.
[g] ND: not detected.

VRX-480773 as a starting point. Our docking model of overlaying the lower-energy conformations of etravirine and VRX-480773 templates within the NNRTIs binding sites (NNIBS) reveals that most fragments in the structures can superpose well with each other (Fig. 2). They exhibit similar binding patterns with HIV-1 RT (Fig. 2). In this paper, a series of etravirine–VRX-480773 hybrids **3** (Fig. 3), characterized by a 2,6-dimethyl-4-cyanophenoxyl group, a central pyrimidine ring and thioacetanilide moieties, were synthesized and evaluated as novel NNRTIs. Preliminary structure-activity relationships (SARs) and molecular modeling for these hybrids are also discussed.

2. Chemistry

The synthetic route for the target compounds **3a-u** is depicted in Scheme 1. Biaryl ether **5** was obtained by regioselective coupling of 2,6-dimethyl-4-cyanophenol to the 4-position of 2,4-dichloropyrimidine (**4**).[6] Treatment of 2-chloropyrimidine **5** with thiourea yielded 2-mercaptopyrimidine **6**.[7] Further condensation with known intermediates α-bromoacetamide **7a-u**[8] created the desired target compounds with yields of 48–86%.

3. Results and discussion

3.1. Biological activity

The newly synthesized etravirine–VRX-480773 hybrids were evaluated for their anti-HIV activity in MT-4 cell cultures infected with a WT HIV-1 strain (ⅢB), a double mutant HIV-1 strain RES056 (K103N + Y181C) or an HIV-2 strain (ROD). The results were expressed as cytotoxicity (CC_{50}), anti-HIV activity (EC_{50}) and selective index (SI = CC_{50}/EC_{50}). The SI indicates the specificity of the antiviral effect. The results are illustrated in Table 1, and include those of the two FDA approved drugs, delavirdine (DEV) and etravirine (ETV), as the reference standards.

As listed in Table 1, these hybrids (except for compound **3a**) were found to exhibit anti-HIV-1 ⅢB activity in the lower micromolar range (EC_{50} = 0.24–41 μM) with SI values ranging from 1 to > 1225. Compound **3d** was the most potent inhibitor with an EC_{50} value of 0.24 μM against WT HIV-1. This activity was superior to that of the reference compound DEV (EC_{50} = 0.66 μM, SI > 67), but inferior to that of ETV (EC_{50} = 0.0041 μM) and VRX-480773 (EC_{50} = 0.00014 μM[2]). It is worth noting that analogues **3k** (EC_{50} = 0.34 μM, SI > 844) and **3s** (EC_{50} = 0.81 μM, SI = 57) possessed the same inhibitory activity as DEV against WT HIV-1. However, these hybrids lack potency against the double mutant strain RES056 and HIV-2. The preliminary SARs analyses indicated that the substitution pattern on the right wing of the hybrids might play a determinant role in their anti-HIV-1 (ⅢB) activity. All phenyl-substituted hybrids were more potent than the non-substituted parent compound **3a**, regardless of the electronic effect and steric bulk. In the case of di-substitution over mono-substitution of the phenyl ring, 2,4-dichloro-substituted **3g** (EC_{50} = 1.2 μM) showed no marked improvement on the ability to inhibit WT virus compared with 2-chloro (**3d**) and 4-chloro (**3f**) analogues (EC_{50} = 0.24 and 3.9 μM, respectively), with the exception of a 10-fold boost in activity achieved when a second methyl group was introduced in compound **3s**. The inhibitory potency was higher for the *ortho*-substituted derivatives (**3d** and **3k**) than for the *para*-substituted analogues (**3f** and **3m**) that in turn was more active than the *meta*-substituted congeners (**3e** and **3l**). For the compounds with a mono-substituent at the C-4 position of the phenyl ring, the electron-withdrawing groups (**3j**, **3m**, **3f** and **3n**) seem to be more advantageous than the electron-donating substituents (**3r** and

3t). Derivatives with hydrophobic groups (**3n** and **3r**) were more potent than analogs with hydrophilic substituents (**3p** and **3u**).

Druglike physicochemical property (Table 1) of these hybrids were predicted by using software ACD[11] or ChemAxon[12], respectively. As for pKa, log P and molar refractivity (MR), the patterns of hybrids were similar to the parent etravirine and VRX-480773. Furthermore, molecular polar surface area (PSA) values were calculated by using ChemAxon software as a prediction of oral bioavailability. The values for all compounds (except for compounds **3p** and **3s**) less than 140 Å[2].[13]

With the aim to verify their binding target, three selected title compounds (**3d**, **3k**, and **3s**) were assessed in enzyme assays[14,15] against highly purified recombinant HIV-1 RT using poly(rA)/oligo(dT)$_{16}$ as template and primer, nevirapine (NVP) and efavirenz (EFV) as reference (Table 2). All the tested compounds showed moderate inhibitory activity against WT HIV-1 RT. The results confirmed the SAR information obtained in antiviral evaluation in MT-4 cells. As an example, compound **3d** still displayed the highest inhibitory activity against WT HIV-1 RT with IC_{50} value of 0.473 μM, which was higher than nevirapine (NVP, IC_{50} = 0.807 μM), but lower than efavirenz (EFV, IC_{50} = 0.022 μM). The regression analysis (Fig. 4) of pEC_{50} and pIC_{50} (most of data removed for clarity) with a correlation factor of 0.87 indicated that these hybrids bind to HIV-1 RT.

Table 2

Inhibitory activity of representative hybrids against WT HIV-1 RT[a]

Compounds	IC_{50}[b] (μM)
3d	0.473 ± 0.155
3k	1.169 ± 0.216
3s	2.775 ± 0.117
NVP	0.807 ± 0.326
EFV	0.022 ± 0.006

[a] Data represent the mean values of at least two separate experiments.

[b] IC_{50}: inhibitory concentration required to inhibit biotin deoxyuridine triphosphate (biotin-dUTP) incorporation into the HIV-1 RT by 50%.

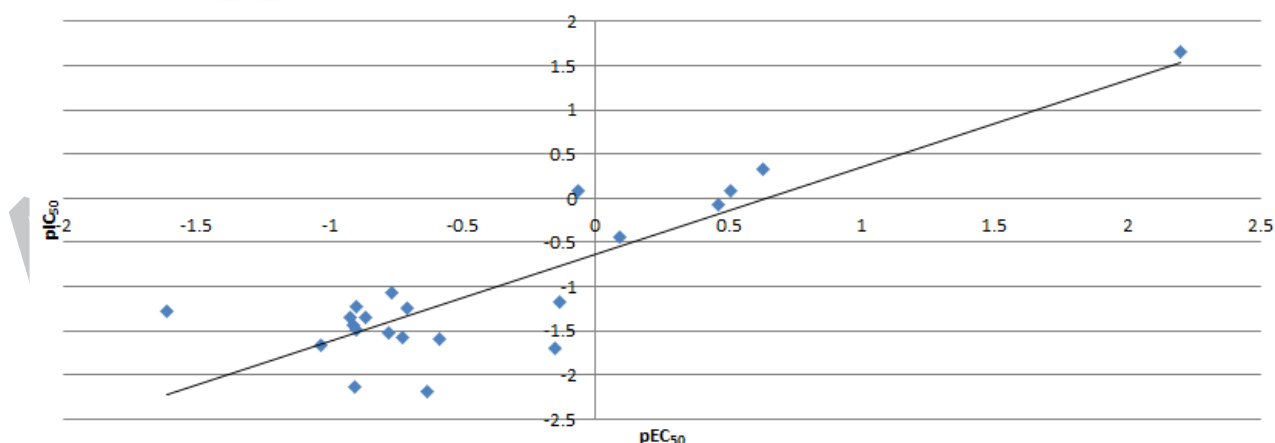**Figure 4.** Regression analysis pEC_{50} and pIC_{50}

Furthermore, we also performed time-of-addition experiments in MT-4 cells in which the test compounds were added at different time points after infection of the cell cultures

with WT HIV-1. Reference compounds with known mode of action were included such as NRTI AZT that inhibits HIV RT (0-3 h post infection), NNRTIs NVP and ETV that inhibits HIV

RT (3-5 h post infection), the diketo acid EVG that inhibits the strand transfer step of the integration (7-8 h post-infection) and WP7-5 that is an inhibitor of transcription (10-16 h post-infection). Addition of the etravirine–VRX-480773 hybrids, **3d**, **3k** and **3s**, all can be postponed for 3-5 h post-infection, coinciding with the process of reverse transcription, which is also confirmed by a similar behavior of the NNRTIs NVP and ETV in the experiments.

3.2. Molecular simulation

To investigate the HIV-1 inhibitory potencies of the newly synthesized etravirine–VRX-480773 hybrids at a molecular level, molecular simulation was carried out. This was done by docking the representative compound **3a** into the NNIBS of WT HIV-1 RT (PDB code: 3C6T)[16] using a Base-Builder program and Surflex-Dock program interfaced with SYBYL-X 1.2. The results are shown in Fig. 5. The hybrid **3a** was predicted to bind with NNIBS in a "U" mode. Notable features include: (1) the left phenyl ring fitted into the aromatic-rich binding pocket, which was surrounded by the aromatic side chains of amino acid residues Tyr181, Tyr188 and Trp229, and exhibited π–π stacking interaction with these residues; (2) the right aromatic ring extended to the enzyme/water interfaces and made lipophilic interactions with the amino acids Phe227, Pro236 and Tyr318; (3) a hydrogen bond was formed between the NH group of the C2 side chain of hybrid **3a** and the backbone C=O of Lys103, improving the affinity between RT and inhibitors.
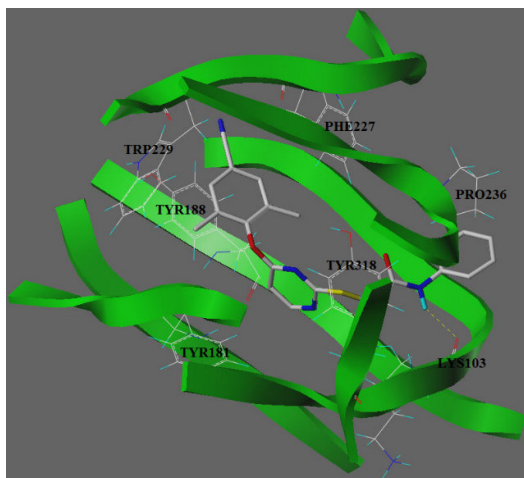

Figure 5. Predicted binding mode of the representative hybrid **3a** in NNIBS of WT HIV-1 RT (PDB code: 3C6T).

In summary, the computational modeling study was helpful to better understand the interactions between the hybrids and HIV-1 RT. The molecular binding model of compounds **3a** provided critical insights for further development of new hybrid molecules.

4. Conclusion

Based on a structure-guided molecular hybridization approach, we designed and synthesized a novel series of etravirine–VRX-480773 hybrids as potent HIV-1 NNRTIs. These hybrids were assessed for their anti-HIV-1 activity in MT-4 cell cultures. Most compounds (except for compound **3a**) exhibited significant potency against WT HIV-1 strain (IIIB) at micromolar concentrations (EC_{50} = 0.24–41 μM). Among them,

compound **3d** displayed the highest activity with an EC_{50} value of 0.24 μM and SI > 1225. Taking full use of the information from SAR analyses and molecular modeling calculations, further optimization of this series of hybrids to improve their drug resistance profiles are ongoing and will be reported in due course.

5. Material and methods

5.1. Chemistry

Chemical reagents and solvents, purchased from commercial sources, were of analytical grade and were used without further purification. All air-sensitive reactions were run under a nitrogen atmosphere. All the reactions were monitored by TLC on pre-coated silica gel G plates at 254 nm under a UV lamp using ethyl acetate/hexane as eluent. Column chromatography separations were performed with silica gel (300–400 mesh). Melting points were measured on a SGW X-1 microscopic melting point apparatus. ^1H NMR and ^{13}C NMR spectra were recorded on a Bruker AV400 MHz spectrometer in DMSO-d_6. Chemical shifts were reported in δ (ppm) units relative to the internal standard tetramethylsilane (TMS). IR analysis were carried out on a JASCO FT/IR-4200 series. Mass spectra and HRMS were obtained on a Waters Quattro Micromass instrument and Bruker solari X-70 FT-MS instrument, respectively, using electrospray ionization (ESI) techniques. The purities of target compounds were ≥ 95%, measured by HPLC, performed on an Agilent 1200 HPLC system with UV detector and Agilent Eclipse Plus C_{18} column (150 × 4.6 mm, 5 μm), eluting with a mixture of solvents H_2O (A) and CH_3CN (B) from V_A: V_B = 90:10 to 10:90. Peaks were detected at λ 254 nm with a flow rate of 1.0 mL/min.

5.2. Preparation of 4-((2-chloropyrimidin-4-yl)oxy)-3,5-dimethylbenzonitrile (5)

Sodium hydride (2.20 g, 55 mmoL) was added in portions to a solution of 4-hydroxy-3,5-dimethylbenzonitrile (7.35 g, 50 mmoL) in anhydrous THF (100 mL) at room temperature.[6] The resulting solution was stirred for 10 min, then 2,4-dichloropyrimidine (**4**) (7.40 g, 50 mmoL) was added. The reaction mixture was heated to 40 °C and maintained for 6 h. The progress of the reaction was monitored by TLC. After completion of the reaction, the reaction mixture was cooled to RT, poured into vigorously stirred ice water (800 mL), and filtered; the precipitated solid was washed with chilled water, and dried at 50 °C under vacuum. The corresponding crude product was recrystallized from DMF to afford pure **5** (71% yield) as white crystals. Mp 230.3–230.9 °C; ^1H NMR (400 MHz, DMSO-d_6) δ = 2.08 (s, 6H, 2CH_3), 7.28 (d, J = 5.6 Hz, 1H, pyrimidine H_5), 7.71 (s, 2H, Ph$H_{3,5}$), 8.67 (d, J = 5.6 Hz, 1H, pyrimidine H_6); ^{13}C NMR (100 MHz, DMSO-d_6) δ = 15.79, 107.14, 109.27, 118.50, 132.49, 132.98, 152.34, 159.29, 162.13, 168.63; MS (ESI+) m/z 260 (M+H)$^+$; HRMS calcd for $C_{13}H_{10}ClN_3O$ [M+Na]$^+$: 282.0410, found: 282.0409.

5.3. Preparation of 4-((2-mercaptopyrimidin-4-yl)oxy)-3,5-dimethylbenzonitrile (6)

4-((2-chloropyrimidin-4-yl)oxy)-3,5-dimethylbenzonitrile (**5**) (4.26 g, 16.4 mmoL), thiourea (1.88 g, 24.6 mmoL) and ethanol (75 mL) were boiled under reflux for 4.5 h.[7] After the mixture was cooled, the precipitate was collected by filtration, washed with EtOH (2 × 10 mL) and dried at 50 °C under vacuum to give compound 4-((2-mercaptopyrimidin-4-yl)oxy)-3,5-dimethylbenzonitrile (**6**) as a white solid. Yield: 77%. Mp 290.2–290.5 °C; ^1H NMR (400 MHz, DMSO-d_6) δ = 2.09 (s,

6H, 2C*H*$_3$), 6.61 (d, *J* = 6.8 Hz, 1H, pyrimidine *H*$_5$), 7.69 (s, 2H, Ph*H*$_{3,5}$), 7.99 (d, *J* = 6.8 Hz, 1H, pyrimidine *H*$_6$); ^{13}C NMR (100 MHz, DMSO-*d*$_6$) δ = 15.94, 98.03, 108.89, 118.64, 132.49, 132.73, 149.25, 152.71, 166.13, 182.38; MS (ESI+) *m/z* 258 (M+H)$^+$; HRMS calcd for C$_{13}$H$_{11}$N$_3$OS [M+H]$^+$: 258.0701, found: 258.0698.

5.4. General procedure for the preparation of 3a-u

Potassium tert-butoxide (0.0589 g, 0.525 mmoL) was added to a solution of 4-((2-mercaptopyrimidin-4-yl)oxy)-3,5-dimethylbenzonitrile (**6**) (0.1287 g, 0.50 mmoL) in 1.5 mL of anhydrous DMF. The mixture was stirred for 30 min before 0.50 mmoL of a known intermediate α-bromoacetamide **7a-u**[8] was added dropwise as a solution in 0.6 mL of anhydrous DMF and the reaction was stirred at room temperature for 1 h. The reaction was followed by TLC until its completion and water (21 mL) was added. The mixture was extracted with ethyl acetate (3 × 20 mL), washed with water (3 × 10 mL) and brine (3 × 10 mL), and dried over Na$_2$SO$_4$ to give the corresponding crude product, which was purified by flash column chromatography to afford compounds **3a-u**.

5.4.1. 2-((4-(4-Cyano-2,6-dimethylphenoxy)pyrimidin-2-yl)thio)-*N*-phenylacetamide (3a)

Yield 76%; white solid, mp 211.2–211.6 °C; ^{1}H NMR (400 MHz, DMSO-*d*$_6$) δ = 1.98 (s, 6H, 2C*H*$_3$), 3.78 (s, 2H, C*H*$_2$), 6.92 (d, *J* = 5.6 Hz, 1H, pyrimidine *H*$_5$), 7.07 (m, 1H, Ph'*H*$_4$), 7.31 (m, 4H, Ph*H*$_{3,5}$ + Ph'*H*$_{3,5}$), 7.54 (d, *J* = 6.4 Hz, 2H, Ph'*H*$_{2,6}$), 8.54 (d, *J* = 5.6 Hz, 1H, pyrimidine *H*$_6$), 9.91 (s, 1H, N*H*); ^{13}C NMR (100 MHz, DMSO-*d*$_6$) δ = 15.74, 35.21, 103.18, 108.78, 118.59, 118.76, 123.21, 128.75, 132.14, 132.51, 139.27, 152.36, 159.90, 165.26, 166.95, 170.75; IR (KBr): $\tilde{v}$ = 3387 (s; *v*(N-H)), 2219 (s; *v*(C≡N)), 1709 cm^{-1} (s; *v*(C=O)); MS (ESI+) *m/z* 391 (M+H)$^+$; HRMS calcd for C$_{21}$H$_{18}$N$_4$O$_2$S [M+Na]$^+$: 413.1048, found: 413.1042; HPLC: t$_R$ = 8.21 min, 99.2%.

5.4.2. 2-((4-(4-Cyano-2,6-dimethylphenoxy)pyrimidin-2-yl)thio)-*N*-(3-fluorophenyl)acetamide (3b)

Yield 75%; white solid, mp 204.6–205.4 °C; ^{1}H NMR (400 MHz, DMSO-*d*$_6$) δ = 1.97 (s, 6H, 2C*H*$_3$), 3.78 (s, 2H, C*H*$_2$), 6.88-6.94 (m, 2H, pyrimidine *H*$_5$ + Ph'*H*$_4$), 7.24 (m, 1H, Ph'*H*$_5$), 7.34-7.38 (m, 3H, Ph*H*$_{3,5}$ + Ph'*H*$_6$), 7.51 (d, *J* = 11.2 Hz, 1H, Ph'*H*$_2$), 8.54 (d, *J* = 5.6 Hz, 1H, pyrimidine *H*$_6$), 10.11 (s, 1H, N*H*); ^{13}C NMR (100 MHz, DMSO-*d*$_6$) δ = 15.72, 35.20, 103.20, 105.40 (d, $J_{C\text{-}C\text{-}F}$ = 26.3 Hz), 108.77, 109.54 (d, $J_{C\text{-}C\text{-}F}$ = 21.0 Hz), 114.52 (d, $J_{C4\text{-}F}$ = 2.3 Hz), 118.54, 130.43 (d, $J_{C3\text{-}F}$ = 9.3 Hz), 132.10, 132.45, 140.90 (d, $J_{C3\text{-}F}$ = 10.9 Hz), 152.33, 159.92, 163.35 (d, $J_{C\text{-}F}$ = 239.9 Hz), 165.61, 166.95, 170.63; MS (ESI+) *m/z* 456 (M+Na)$^+$; HRMS calcd for C$_{21}$H$_{17}$FN$_4$O$_2$S [M+H]$^+$: 409.1134, found: 409.1128; HPLC: t$_R$ = 10.25 min, 96.9%.

5.4.3. 2-((4-(4-Cyano-2,6-dimethylphenoxy)pyrimidin-2-yl)thio)-*N*-(4-fluorophenyl)acetamide (3c)

Yield 83%; white solid, mp 206.1–206.5 °C; ^{1}H NMR (400 MHz, DMSO-*d*$_6$) δ = 1.99 (s, 6H, 2C*H*$_3$), 3.78 (s, 2H, C*H*$_2$), 6.92 (d, *J* = 5.6 Hz, 1H, pyrimidine *H*$_5$), 7.15 (t, *J* = 8.6 Hz, 2H, Ph'*H*$_{3,5}$), 7.40 (s, 2H, Ph*H*$_{3,5}$), 7.54-7.57 (m, 2H, Ph'*H*$_{2,6}$), 8.54 (d, *J* = 5.6 Hz, 1H, pyrimidine *H*$_6$), 9.97 (s, 1H, N*H*); ^{13}C NMR (100 MHz, DMSO-*d*$_6$) δ = 15.71, 35.09, 103.18, 108.73, 115.40 (d, $J_{C\text{-}C\text{-}F}$ = 22.1 Hz), 118.56, 120.44 (d, $J_{C3\text{-}F}$ = 7.7 Hz), 132.14, 132.50, 135.65 (d, $J_{C4\text{-}F}$ = 2.4 Hz), 152.36, 156.70 (d, $J_{C\text{-}F}$ = 237.8 Hz), 159.89, 165.16, 166.94, 170.69; MS (ESI+) *m/z* 409 (M+H)$^+$; HRMS calcd for C$_{21}$H$_{17}$FN$_4$O$_2$S [M+H]$^+$: 409.1134, found: 409.1135; HPLC: t$_R$ = 10.09 min, 97.7%.

5.4.4. *N*-(2-Chlorophenyl)-2-((4-(4-cyano-2,6-dimethylphenoxy)pyrimidin-2-yl)thio)acetamide (3d)

Yield 84%; white solid, mp 170.0–170.8 °C; ^{1}H NMR (400 MHz, DMSO-*d*$_6$) δ = 2.02 (s, 6H, 2C*H*$_3$), 3.93 (s, 2H, C*H*$_2$), 6.95 (d, *J* = 5.6 Hz, 1H, pyrimidine *H*$_5$), 7.17 (t, *J* = 7.6 Hz, 1H, Ph'*H*$_4$), 7.33 (t, *J* = 7.8 Hz, 1H, Ph'*H*$_5$), 7.47 (d, *J* = 8.0 Hz, 1H, Ph'*H*$_3$), 7.56 (s, 2H, Ph*H*$_{3,5}$), 7.82 (d, *J* = 8.4 Hz, 1H, Ph'*H*$_6$), 8.58 (d, *J* = 5.6 Hz, 1H, pyrimidine *H*$_6$), 9.48 (s, 1H, N*H*); ^{13}C NMR (100 MHz, DMSO-*d*$_6$) δ = 15.72, 34.91, 103.54, 108.81, 118.48, 124.32, 124.84, 125.87, 127.52, 129.47, 132.25, 132.66, 134.69, 152.41, 160.02, 166.24, 167.02, 170.31; MS (ESI+) *m/z* 458 (M+Na)$^+$; HRMS calcd for C$_{21}$H$_{17}$ClN$_4$O$_2$S [M+Na]$^+$: 447.0658, found: 447.0658; HPLC: t$_R$ = 10.31 min, 96.3%.

5.4.5. *N*-(3-Chlorophenyl)-2-((4-(4-cyano-2,6-dimethylphenoxy)pyrimidin-2-yl)thio)acetamide (3e)

Yield 78%; white solid, mp 200.0–200.8 °C; ^{1}H NMR (400 MHz, DMSO-*d*$_6$) δ = 1.97 (s, 6H, 2C*H*$_3$), 3.77 (s, 2H, C*H*$_2$), 6.93 (d, *J* = 5.6 Hz, 1H, pyrimidine *H*$_5$), 7.12 (d, *J* = 7.2 Hz, 1H, Ph'*H*$_4$), 7.34-7.36 (m, 4H, Ph*H*$_{3,5}$ + Ph'*H*$_{5,6}$), 7.76 (s, 1H, Ph'*H*$_2$), 8.54 (d, *J* = 5.6 Hz, 1H, pyrimidine *H*$_6$), 10.09 (s, 1H, N*H*); ^{13}C NMR (100 MHz, DMSO-*d*$_6$) δ = 15.73, 35.19, 103.20, 108.75, 117.15, 118.22, 118.51, 122.90, 130.45, 132.09, 132.45, 133.13, 140.65, 152.32, 159.92, 165.63, 166.93, 170.61; MS (ESI+) *m/z* 425 (M+H)$^+$; HRMS calcd for C$_{21}$H$_{17}$ClN$_4$O$_2$S [M+Na]$^+$: 447.0658, found: 447.0646; HPLC: t$_R$ = 9.47 min, 97.4%.

5.4.6. *N*-(4-Chlorophenyl)-2-((4-(4-cyano-2,6-dimethylphenoxy)pyrimidin-2-yl)thio)acetamide (3f)

Yield 84%; white solid, mp 176.0–176.4 °C; ^{1}H NMR (400 MHz, DMSO-*d*$_6$) δ = 1.98 (s, 6H, 2C*H*$_3$), 3.77 (s, 2H, C*H*$_2$), 6.92 (d, *J* = 5.6 Hz, 1H, pyrimidine *H*$_5$), 7.35-7.37 (m, 4H, Ph*H*$_{3,5}$ + Ph'*H*$_{3,5}$), 7.55-7.57 (d, *J* = 8.8 Hz, 2H, Ph'*H*$_{2,6}$), 8.53 (d, *J* = 5.6 Hz, 1H, pyrimidine *H*$_6$), 10.05 (s, 1H, N*H*); ^{13}C NMR (100 MHz, DMSO-*d*$_6$) δ = 15.77, 35.21, 103.26, 108.78, 118.63, 120.35, 126.77, 128.70, 132.20, 132.54, 138.23, 152.41, 159.96, 165.48, 167.00, 170.68; MS (ESI+) *m/z* 447 (M+Na)$^+$; HRMS calcd for C$_{21}$H$_{17}$ClN$_4$O$_2$S [M+H]$^+$: 425.0839, found: 425.0838; HPLC: t$_R$ = 10.81 min, 96.0%.

5.4.7. 2-((4-(4-Cyano-2,6-dimethylphenoxy)pyrimidin-2-yl)thio)-*N*-(2,4-dichlorophenyl)acetamide (3g)

Yield 77%; white solid, mp 188.8–189.5 °C; ^{1}H NMR (400 MHz, DMSO-*d*$_6$) δ = 2.02 (s, 6H, 2C*H*$_3$), 3.93 (s, 2H, C*H*$_2$), 6.94 (d, *J* = 5.6 Hz, 1H, pyrimidine *H*$_5$), 7.41 (d, *J* = 8.4 Hz, 1H, Ph'*H*$_5$), 7.56 (s, 2H, Ph*H*$_{3,5}$), 7.64 (s, 1H, Ph'*H*$_3$), 7.83 (d, *J* = 8.8 Hz, 1H, Ph'*H*$_6$), 8.57 (d, *J* = 5.6 Hz, 1H, pyrimidine *H*$_6$), 9.56 (s, 1H, N*H*); ^{13}C NMR (100 MHz, DMSO-*d*$_6$) δ = 15.73, 34.90, 103.53, 108.78, 118.46, 125.34, 125.72, 127.62, 128.86, 128.92, 132.26, 132.65, 133.93, 152.42, 160.01, 166.43, 167.01, 170.31; MS (ESI+) *m/z* 481 (M+Na)$^+$; HRMS calcd for C$_{21}$H$_{16}$Cl$_2$N$_4$O$_2$S [M+Na]$^+$: 481.0269, found: 481.0265; HPLC: t$_R$ = 12.21 min, 97.6%.

5.4.8 2-((4-(4-Cyano-2,6-dimethylphenoxy)pyrimidin-2-yl)thio)-*N*-(3,4-dichlorophenyl)acetamide (3h)

Yield 85%; white solid, mp 203.6–204.3 °C; ^{1}H NMR (400 MHz, DMSO-*d*$_6$) δ = 1.98 (s, 6H, 2C*H*$_3$), 3.77 (s, 2H, C*H*$_2$), 6.94 (d, *J* = 5.6 Hz, 1H, pyrimidine *H*$_5$), 7.36 (s, 2H, Ph*H*$_{3,5}$), 7.42 (d, *J* = 8.8 Hz, 1H, Ph'*H*$_5$), 7.56 (d, *J* = 8.8 Hz, 1H, Ph'*H*$_6$), 7.90 (s, 1H, Ph'*H*$_2$), 8.54 (d, *J* = 5.6 Hz, 1H, pyrimidine *H*$_6$), 10.19 (s, 1H, N*H*); ^{13}C NMR (100 MHz, DMSO-*d*$_6$) δ = 15.71, 35.18, 103.23, 108.73, 118.49, 118.79, 119.95, 124.62, 130.71, 131.06, 132.12, 132.44, 139.25, 152.34, 159.93, 165.78, 166.94, 170.53; MS (ESI+) *m/z* 481 (M+Na)$^+$; HRMS calcd for C$_{21}$H$_{16}$Cl$_2$N$_4$O$_2$S [M+Na]$^+$: 481.0269, found: 481.0262; HPLC:

t_R = 11.46 min, 97.5%.

5.4.9. 2-((4-(4-Cyano-2,6-dimethylphenoxy)pyrimidin-2-yl)thio)-*N*-(3,5-dichlorophenyl)acetamide (3i)

Yield 84%; white solid, mp 226.9–227.7 °C; ^{1}H NMR (400 MHz, DMSO-d_6) δ = 1.97 (s, 6H, 2CH_3), 3.75 (s, 2H, CH_2), 6.94 (d, J = 5.6 Hz, 1H, pyrimidine H_5), 7.29-7.33 (m, 3H, Ph$H_{3,5}$ + PhH_4), 7.58 (s, 2H, Ph$H_{2,6}$), 8.54 (d, J = 5.6 Hz, 1H, pyrimidine H_6), 10.22 (s, 1H, NH); ^{13}C NMR (100 MHz, DMSO-d_6) δ = 15.71, 35.22, 103.25, 108.73, 116.90, 118.40, 122.49, 132.09, 132.40, 134.19, 141.44, 152.31, 159.96, 165.97, 166.94, 170.49; MS (ESI+) *m/z* 481 (M+Na)$^+$; HRMS calcd for $C_{21}H_{16}Cl_2N_4O_2S$ [M+H]$^+$: 459.0449, found: 459.0434; HPLC: t_R = 11.78 min, 98.1%.

5.4.10. *N*-(4-Bromophenyl)-2-((4-(4-cyano-2,6-dimethylphenoxy)pyrimidin-2-yl)thio)acetamide (3j)

Yield 86%; white solid, mp 160.7–161.5 °C; ^{1}H NMR (400 MHz, DMSO-d_6) δ = 1.98 (s, 6H, 2CH_3), 3.78 (s, 2H, CH_2), 6.92 (d, J = 5.6 Hz, 1H, pyrimidine H_5), 7.38 (s, 2H, Ph$H_{3,5}$), 7.48-7.53 (m, 4H, Ph$H_{2,3,5,6}$), 8.53 (d, J = 5.6 Hz, 1H, pyrimidine H_6), 10.06 (s, 1H, NH); ^{13}C NMR (100 MHz, DMSO-d_6) δ = 15.75, 35.22, 103.22, 108.76, 114.73, 118.60, 120.69, 131.58, 132.17, 132.51, 138.62, 152.38, 159.93, 165.48, 166.96, 170.65; MS (ESI+) *m/z* 469 (M+H)$^+$; HRMS calcd for $C_{21}H_{17}BrN_4O_2S$ [M+H]$^+$: 469.0334, found: 469.0338; HPLC: t_R = 11.05 min, 97.1%.

5.4.11. 2-((4-(4-Cyano-2,6-dimethylphenoxy)pyrimidin-2-yl)thio)-*N*-(2-nitrophenyl)acetamide (3k)

Yield 85%; yellow solid, mp 180.9–181.5 °C; ^{1}H NMR (400 MHz, DMSO-d_6) δ = 1.99 (s, 6H, 2CH_3), 3.89 (s, 2H, CH_2), 6.96 (d, J = 5.6 Hz, 1H, pyrimidine H_5), 7.36 (t, J = 7.0 Hz, 1H, PhH_4), 7.53 (s, 2H, Ph$H_{3,5}$), 7.75 (t, J = 6.4 Hz, 1H, PhH_5), 7.97-8.05 (m, 2H, Ph$H_{3,6}$), 8.57 (d, J = 5.6 Hz, 1H, pyrimidine H_6), 10.52 (s, 1H, NH); ^{13}C NMR (100 MHz, DMSO-d_6) δ = 15.69, 35.14, 103.71, 108.81, 118.53, 123.79, 124.84, 125.36, 132.10, 132.29, 132.65, 134.84, 139.83, 152.47, 160.07, 166.43, 167.10, 169.92; MS (ESI+) *m/z* 458 (M+Na)$^+$; HRMS calcd for $C_{21}H_{17}N_5O_4S$ [M+Na]$^+$: 458.0899, found: 458.0887; HPLC: t_R = 10.85 min, 97.3%.

5.4.12. 2-((4-(4-Cyano-2,6-dimethylphenoxy)pyrimidin-2-yl)thio)-*N*-(3-nitrophenyl)acetamide (3l)

Yield 84%; light yellow solid, mp 192.8–193.5 °C; ^{1}H NMR (400 MHz, DMSO-d_6) δ = 1.96 (s, 6H, 2CH_3), 3.79 (s, 2H, CH_2), 6.94 (d, J = 5.6 Hz, 1H, pyrimidine H_5), 7.28 (s, 2H, Ph$H_{3,5}$), 7.63 (t, J = 8.0 Hz, 1H, PhH_5), 7.82 (d, J = 7.6 Hz, 1H, PhH_6), 7.93 (d, J = 8.0 Hz, 1H, PhH_4), 8.54-8.55 (m, 2H, pyrimidine H_6 + PhH_2), 10.36 (s, 1H, NH); ^{13}C NMR (100 MHz, DMSO-d_6) δ = 15.70, 35.20, 103.25, 108.63, 112.80, 117.78, 118.47, 124.66, 130.25, 132.11, 132.41, 140.33, 148.01, 152.37, 159.95, 165.97, 166.98, 170.58; MS (ESI+) *m/z* 436 (M+H)$^+$; HRMS calcd for $C_{21}H_{17}N_5O_4S$ [M+H]$^+$: 436.1079, found: 436.1070; HPLC: t_R = 9.98 min, 96.4%.

5.4.13. 2-((4-(4-Cyano-2,6-dimethylphenoxy)pyrimidin-2-yl)thio)-*N*-(4-nitrophenyl)acetamide (3m)

Yield 85%; white solid, mp 208.7–209.5 °C; ^{1}H NMR (400 MHz, DMSO-d_6) δ = 1.97 (s, 6H, 2CH_3), 3.82 (s, 2H, CH_2), 6.94 (d, J = 5.6 Hz, 1H, pyrimidine H_5), 7.34 (s, 2H, Ph$H_{3,5}$), 7.74 (d, J = 8.8 Hz, 2H, Ph$H_{2,6}$), 8.23 (d, J = 9.2 Hz, 2H, Ph$H_{3,5}$), 8.54 (d, J = 5.6 Hz, 1H, pyrimidine H_6), 10.50 (s, 1H, NH); ^{13}C NMR (100 MHz, DMSO-d_6) δ = 15.69, 35.37, 103.26, 108.69, 118.44, 118.54, 125.05, 132.08, 132.47, 142.16, 145.29, 152.32, 159.93, 166.20, 166.96, 170.49; MS (ESI+) *m/z* 458 (M+Na)$^+$; HRMS calcd for $C_{21}H_{17}N_5O_4S$ [M+H]$^+$: 436.1079, found: 436.1061; HPLC: t_R = 10.04 min, 97.2%.

5.4.14. 2-((4-(4-Cyano-2,6-dimethylphenoxy)pyrimidin-2-yl)thio)-*N*-(4-cyanophenyl)acetamide (3n)

Yield 82%; white solid, mp 209.0–209.4 °C; ^{1}H NMR (400 MHz, DMSO-d_6) δ = 1.96 (s, 6H, 2CH_3), 3.79 (s, 2H, CH_2), 6.93 (d, J = 5.6 Hz, 1H, pyrimidine H_5), 7.31 (s, 2H, Ph$H_{3,5}$), 7.68 (d, J = 8.4 Hz, 2H, Ph$H_{3,5}$), 7.77 (d, J = 8.4 Hz, 2H, Ph$H_{2,6}$), 8.53 (d, J = 5.6 Hz, 1H, pyrimidine H_6), 10.32 (s, 1H, NH); ^{13}C NMR (100 MHz, DMSO-d_6) δ = 15.77, 35.38, 103.33, 105.02, 108.76, 118.63, 118.88, 119.24, 132.18, 132.51, 133.42, 143.41, 152.41, 160.01, 166.13, 167.04, 170.59; MS (ESI+) *m/z* 438 (M+Na)$^+$; HRMS calcd for $C_{22}H_{17}N_5O_2S$ [M+H]$^+$: 416.1181, found: 416.1170; HPLC: t_R = 9.57 min, 98.3%.

5.4.15. 2-((4-(4-Cyano-2,6-dimethylphenoxy)pyrimidin-2-yl)thio)-*N*-(4-cyano-2-fluorophenyl)acetamide (3o)

Yield 85%; white solid, mp 217.7–218.2 °C; ^{1}H NMR (400 MHz, DMSO-d_6) δ = 1.98 (s, 6H, 2CH_3), 3.88 (s, 2H, CH_2), 6.94 (d, J = 5.6 Hz, 1H, pyrimidine H_5), 7.35 (s, 2H, Ph$H_{3,5}$), 7.66 (d, J = 8.4 Hz, 1H, PhH_3), 7.87 (d, J = 11.2 Hz, 1H, PhH_5), 8.26 (t, J = 8.2 Hz, 1H, PhH_6), 8.53 (d, J = 5.6 Hz, 1H, pyrimidine H_6), 10.10 (s, 1H, NH); ^{13}C NMR (100 MHz, DMSO-d_6) δ = 15.81, 35.35, 103.41, 105.67 (d, J_{C3-F} = 9.5 Hz), 108.64, 118.09, 118.47, 119.44 (d, J_{C-C-F} = 23.2 Hz), 121.90 (d, J_{C-C-F} = 22.0 Hz), 129.60 (d, J_{C4-F} = 2.9 Hz), 131.68 (d, J_{C3-F} = 11.0 Hz), 132.24, 132.51, 149.92 (d, J_{C-F} = 246.0 Hz), 152.46, 159.99, 166.83, 167.05, 170.59; MS (ESI+) *m/z* 456 (M+Na)$^+$; HRMS calcd for $C_{22}H_{16}FN_5O_2S$ [M+H]$^+$: 434.1087, found: 434.1071; HPLC: t_R = 10.15 min, 97.0%.

5.4.16. 2-((4-(4-Cyano-2,6-dimethylphenoxy)pyrimidin-2-yl)thio)-*N*-(4-sulfamoylphenyl)acetamide (3p)

Yield 77%; white solid, mp 250.9–251.5 °C; ^{1}H NMR (400 MHz, DMSO-d_6) δ = 1.97 (s, 6H, 2CH_3), 3.82 (s, 2H, CH_2), 6.93 (d, J = 5.6 Hz, 1H, pyrimidine H_5), 7.28 (s, 2H, NH_2), 7.38 (s, 2H, Ph$H_{3,5}$), 7.68 (d, J = 8.8 Hz, 2H, Ph$H_{2,6}$), 7.77 (d, J = 8.8 Hz 2H, Ph$H_{3,5}$), 8.54 (d, J = 5.6 Hz, 1H, pyrimidine H_6), 10.28 (s, 1H, NH); ^{13}C NMR (100 MHz, DMSO-d_6) δ = 15.74, 35.27, 103.23, 108.80, 118.35, 118.59, 126.70, 132.15, 132.52, 138.35, 142.07, 152.35, 159.94, 165.92, 166.93, 170.56; MS (ESI+) *m/z* 492 (M+Na)$^+$; HRMS calcd for $C_{21}H_{19}N_5O_4S_2$ [M+H]$^+$: 470.0957, found: 470.0954; HPLC: t_R = 7.92 min, 97.6%.

5.4.17. 2-((4-(4-Cyano-2,6-dimethylphenoxy)pyrimidin-2-yl)thio)-*N*-(o-tolyl)acetamide (3q)

Yield 84%; white solid, mp 167.6–168.4 °C; ^{1}H NMR (400 MHz, DMSO-d_6) δ = 2.05 (s, 6H, 2CH_3), 2.14 (s, 3H, CH_3), 3.92 (s, 2H, CH_2), 6.91 (d, J = 5.6 Hz, 1H, pyrimidine H_5), 7.07 (t, J = 7.0 Hz, 1H, PhH_4), 7.13-7.20 (m, 2H, Ph$H_{5,6}$), 7.40 (d, J = 7.6 Hz, 1H, PhH_3), 7.60 (s, 2H, Ph$H_{3,5}$), 8.56 (d, J = 5.6 Hz, 1H, pyrimidine H_6), 9.33 (s, 1H, NH); ^{13}C NMR (100 MHz, DMSO-d_6) δ = 15.79, 17.79, 34.85, 103.36, 108.81, 118.53, 124.38, 125.15, 125.99, 130.38, 131.07, 132.38, 132.74, 136.20, 152.49, 159.97, 165.94, 166.99, 170.68; MS (ESI+) *m/z* 405 (M+H)$^+$; HRMS calcd for $C_{22}H_{20}N_4O_2S$ [M+H]$^+$: 405.1385, found: 405.1374; HPLC: t_R = 10.46 min, 97.2%.

5.4.18. 2-((4-(4-Cyano-2,6-dimethylphenoxy)pyrimidin-2-yl)thio)-*N*-(p-tolyl)acetamide (3r)

Yield 85%; white solid, mp 195.8–196.3 °C; ^{1}H NMR (400 MHz, DMSO-d_6) δ = 1.98 (s, 6H, 2CH_3), 2.26 (s, 3H, CH_3), 3.77 (s, 2H, CH_2), 6.91 (d, J = 5.2 Hz, 1H, pyrimidine H_5), 7.10 (d, J = 7.6 Hz, 2H, Ph$H_{3,5}$), 7.39 (s, 2H, Ph$H_{3,5}$), 7.42 (d, J = 8.0 Hz, 2H, Ph$H_{2,6}$), 8.53 (d, J = 5.6 Hz, 1H, pyrimidine H_6), 9.84 (s, 1H, NH); ^{13}C NMR (100 MHz, DMSO-d_6) δ = 15.76,

20.52, 35.18, 103.20, 108.79, 118.62, 118.80, 129.13, 132.11, 132.19, 132.56, 136.78, 152.39, 159.91, 165.04, 166.96, 170.78; MS (ESI+) m/z 405 (M+H)$^+$; HRMS calcd for $C_{22}H_{20}N_4O_2S$ [M+Na]$^+$: 427.1205, found: 427.1200; HPLC: t_R = 10.62 min, 97.8%.

5.4.19. 2-((4-(4-Cyano-2,6-dimethylphenoxy)pyrimidin-2-yl)thio)-N-(2-methyl-4-sulfamoylphenyl)acetamide (3s)

Yield 84%; white solid, mp 222.8–223.6 ^{o}C; ^{1}H NMR (400 MHz, DMSO-d_6) δ = 2.04 (s, 6H, 2CH_3), 2.25 (s, 3H, CH_3), 3.97 (s, 2H, CH_2), 6.92 (d, J = 5.6 Hz, 1H, pyrimidine H_5), 7.27 (s, 2H, NH_2), 7.59 (s, 2H, Ph$H_{3,5}$), 7.61-7.72 (m, 3H, Ph$H_{3,5,6}$), 8.56 (d, J = 5.6 Hz, 1H, pyrimidine H_6), 9.50 (s, 1H, NH); ^{13}C NMR (100 MHz, DMSO-d_6) δ = 15.78, 17.93, 34.96, 103.37, 108.78, 118.50, 123.39, 123.71, 127.69, 130.64, 132.32, 132.70, 139.34, 139.87, 152.45, 159.97, 166.33, 166.97, 170.56; MS (ESI+) m/z 409 (M+H)$^+$; HRMS calcd for $C_{22}H_{21}N_5O_4S_2$ [M+H]$^+$: 484.1113, found: 484.1115; HPLC: t_R = 8.45 min, 98.4%.

5.4.20. 2-((4-(4-Cyano-2,6-dimethylphenoxy)pyrimidin-2-yl)thio)-N-(4-methoxyphenyl)acetamide (3t)

Yield 86%; white solid, mp 184.5–185.3 ^{o}C; ^{1}H NMR (400 MHz, DMSO-d_6) δ = 1.99 (s, 6H, 2CH_3), 3.73 (s, 3H, CH_3), 3.77 (s, 2H, CH_2), 6.87 (d, J = 8.8 Hz, 2H, Ph$H_{3,5}$), 6.91 (d, J = 5.6 Hz, 1H, pyrimidine H_5), 7.42-7.47 (m, 4H, Ph$H_{3,5}$ + Ph$H_{2,6}$), 8.54 (d, J = 5.6 Hz, 1H, pyrimidine H_6), 9.80 (s, 1H, NH); ^{13}C NMR (100 MHz, DMSO-d_6) δ = 15.74, 35.07, 55.19, 103.17, 108.76, 113.85, 118.60, 120.25, 132.18, 132.47, 132.55, 152.39, 155.14, 159.89, 164.76, 166.95, 170.78; MS (ESI+) m/z 421 (M+H)$^+$; HRMS calcd for $C_{22}H_{20}N_4O_3S$ [M+H]$^+$: 421.1334, found: 421.1332; HPLC: t_R = 9.74 min, 96.9%.

5.4.21. 2-((4-(4-Cyano-2,6-dimethylphenoxy)pyrimidin-2-yl)thio)-N-(4-hydroxyphenyl)acetamide (3u)

Yield 80%; white solid, mp 199.4–200.2 ^{o}C; ^{1}H NMR (400 MHz, DMSO-d_6) δ = 1.99 (s, 6H, 2CH_3), 3.75 (s, 2H, CH_2), 6.69 (d, J = 8.4 Hz, 2H, Ph$H_{3,5}$), 6.91 (d, J = 5.6 Hz, 1H, pyrimidine H_5), 7.32 (d, J = 8.4 Hz, 2H, Ph$H_{2,6}$), 7.43 (s, 2H, Ph$H_{3,5}$), 8.53 (d, J = 5.6 Hz, 1H, pyrimidine H_6), 9.21 (s, 1H, OH), 9.68 (s, 1H, NH); ^{13}C NMR (100 MHz, DMSO-d_6) δ = 15.75, 35.05, 103.15, 108.77, 115.06, 118.61, 120.47, 131.02, 132.19, 132.58, 152.39, 153.25, 159.88, 164.54, 166.94, 170.81; MS (ESI+) m/z 407 (M+H)$^+$; HRMS calcd for $C_{21}H_{18}N_4O_3S$ [M+H]$^+$: 407.1178, found: 407.1167; HPLC: t_R = 8.18 min, 97.9%.

5.5. Anti-HIV activity assay

The anti-HIV activity and cytotoxicity of the compounds 3a-u were evaluated against wild-type HIV-1 strain IIIB, a double RT mutant (K103N + Y181C) HIV-1 strain and HIV-2 strain ROD in MT-4 cell cultures using the 3-(4,5-dimethylthiazol-2-yl)-2,5-diphenyltetrazolium bromide (MTT) method.[17,18] Briefly, virus stocks were titrated in MT-4 cells and expressed as the 50% cell culture infective dose (CCID$_{50}$). MT-4 cells were suspended in culture medium at 1×10^5 cells/mL and infected with HIV at a multiplicity of infection of 0.02. Immediately after viral infection, 100 µL of the cell suspension was placed in each well of a flat-bottomed microtiter tray containing various concentrations of the test compounds. The test compounds were dissolved in DMSO at 50 mM or higher. After 4 days of incubation at 37 °C, the number of viable cells was determined using the MTT method. Compounds were tested in parallel for cytotoxic effects in uninfected MT-4 cells.

5.6. HIV-1 RT assay

Recombinant wild type p66/p51 HIV-1 RT was expressed and purified as previously described.[14] The RT assay was performed with the EnzCheck Reverse Transcriptase Assay kit (Molecular Probes, Invitrogen), as described by the Manufacturer. The assay was based on the dsDNA quantitation reagent PicoGreen. This reagent showed a pronounced increase in fluorescence signal upon binding to dsDNA or RNA-DNA heteroduplexes. Single-stranded nucleic acids generated only minor fluorescence signal enhancement when a sufficiently high dye:base pair ratio was applied.[15] This condition was met in the assay.

A poly(rA) template of approximately 350 bases long, and an oligo(dT)$_{16}$ primer, were annealed in a molar ratio of 1:1.2 (60 min, at room temperature). 52 ng of the RNA/DNA was brought into each well of a 96-well plate in a volume of 20 mL polymerization buffer (60 mM Tris-HCl, 60 mM KCl, 8 mM MgCl$_2$, 13 mM DTT, 100 mM dTTP, pH = 8.1). 5.0 mL of RT enzyme solution, diluted to a suitable concentration in enzyme dilution buffer (50 mM Tris-HCl, 20% glycerol, 2 mM DTT, pH = 7.6), was added. The reaction mixture was incubated at 25 ^{o}C for 40 min and then stopped by the addition of EDTA (15 mM). Heteroduplexes were then detected by addition of PicoGreen. Signals were read using an excitation wavelength of 490 nm and emission detection at 523 nm using a spectrofluorometer (Safire2, Tecan). To test the activity of compounds against RT, 1.0 mL of compound in DMSO was added to each well before the addition of RT enzyme solution. Control wells without compound contained the same amount of DMSO. Results were expressed as relative fluorescence, i. e. the fluorescence signal of the reaction mixed with compound divided by the signal of the same reaction mixed without compound.

5.7. Time-of-addition experiments

Time-of-addition experiments were adapted from Pauwels[19] and Daelemans[20]. Briefly, MT-4 cells were infected with WT HIV-1 at an m.o.i. of 0.5. Following a 1 h adsorption period cells were distributed in a 96-well tray at 45,000 cells/well and incubated at 37°C. Test compounds were added at different times (0, 1, 2, 3, 4, 5, 6, 7, 8, 9, 24, and 25 h) after infection. HIV-1 production was determined at 31 h postinfection *via* a p24 enzyme-linked immunosorbent assay (Perkin Elmer, Brussels, Belgium). Dextran sulfate was used at 12.5 µM, AZT at 1.9 µM, ETV at 0.19 µM, EVG at 0.31 µM, the 6-aminoquinolone derivative WP7-5 at 0.25 µM and the etravirine–VRX-480773 hybrids were added at their 100-fold their EC$_{50}$ concentration obtained in the MT-4/MTT assay.

5.8. Molecular docking

Molecular modeling was performed with the Tripos molecular modeling packages Sybyl-X 1.2. All the molecules for docking were built using standard bond lengths and angles from Sybyl-X 1.2/base Builder and were then optimized using the Tripos force field for 2000 generations two times or more, until the minimized conformers of the ligand were the same. The flexible docking method, called Surflex-Dock[21], docks the ligand automatically into the ligand binding site of the receptor by using a protocol-based approach and an empirically-derived scoring function[22]. The protocol is a computational representation of a putative ligand that binds to the intended binding site and is a unique and essential element of the docking algorithm[23]. The scoring function in Surflex-Dock, which contains hydrophobic, polar, repulsive, entropic, and solvation terms, was trained to estimate the dissociation constant (K$_d$) expressed in -log (K$_d$)^2. Prior to docking, the protein was prepared by removing water molecules, the ligand,

and other unnecessary small molecules from the crystal structure of the ligand–HIV-1 RT complex (PDB code: 3C6T)[16]; simultaneously, polar hydrogen atoms were added to the protein. Surflex-Dock default settings were used for other parameters, such as the number of starting conformations per molecule (set to 0), the size to expand search grid (set to 8 Å), the maximum number of rotatable bonds per molecule (set to 100), and the maximum number of poses per ligand (set to 20). During the docking procedure, all of the single bonds in residue side-chains inside the defined RT binding pocket were regarded as rotatable or flexible, and the ligand was allowed to rotate at all single bonds and move flexibly within the tentative binding pocket. The atomic charges were recalculated using the Kollman all-atom approach for the protein and the Gasteiger-Hückel approach for the ligand. The binding interaction energy was calculated, including van der Waals, electrostatic, and torsional energy terms defined in the Tripos force field. The structure optimization was performed for 20,000 generations using a genetic algorithm, and the 20-best-scoring ligand-protein complexes were kept for further analyses. The -log $(K_d)^2$ values of the 20-best-scoring complexes, which represented the binding affinities of ligand with RT, encompassed a wide scope of functional classes (10^{-2}–10^{-9}). Therefore, only the highest-scoring 3D structural model of the ligand-bound RT was chosen to define the binding interaction[24].

Acknowledgements

References and notes

1 Wu, Z. Y.; Liu, N.; Qin, B.; Huang, L.; Yu, F.; Qian, K.; Morris-Natschke, S. L.; Jiang, S.; Chen, C. H.; Lee, K.; Xie, L. *ChemMedChem* **2014**, *9*, 1546-1555.

2 Zhang, Z. J.; Xu, W.; Koh, Y. H.; Shim, J. H.; Girardet, J. L.; Yeh, L. T.; Hamatake, R. K.; Hong, Z. *Antimicrob. Agents Chemother.* **2007**, *51*, 429-437.

3 Zeng, Z. S.; He, Q. Q.; Liang, Y. H.; Feng, X. Q.; Chen, F. E.; De Clercq, E.; Balzarini, J.; Pannecouque, C. *Bioorg. Med. Chem.* **2010**, *18*, 5039-5047.

4 Yang, S. Q.; Pannecouque, C.; Daelemans, D.; Ma, X. D.; Liu, Y.; Chen, F. E.; De Clercq, E. *Eur. J. Med. Chem.* **2013**, *65*, 134-143.

5 Wu, H. Q.; Yao, J.; He, Q. Q.; Chen, W. X.; Chen, F. E.; Pannecouque, C.; De Clercq, E.; Daelemans, D. *Bioorg. Med. Chem.* **2015**, *23*, 624-631.

6 Kertesz, D. J.; Brotherton-Pleiss, C.; Yang, M.; Wang, Z.; Lin, X.; Qiu, Z.; Hirschfeld, D. R.; Gleason, S.; Mirzadegan, T.; Dunten, P. W.; Harris, S. F.; Villaseñor, A. G.; Hang, J. Q.; Heilek, G. M.; Klumpp, K. *Bioorg. Med. Chem. Lett.* **2010**, *20*, 4215-4218.

7 Brown, D. J.; Mori, K. *Aust. J. Chem.* **1985**, *38*, 467-474.

8 Romines, K. R.; Freeman, G. A.; Schaller, L. T.; Cowan, J. R.; Gonzales, S. S.; Tidwell, J. H.; Andrews, C. W.; Stammers, D. K.; Hazen, R. J.; Ferris, R. G.; Short, S. A.; Chan, J. H.; Boone, L. R. *J. Med. Chem.* **2006**, *49*, 727-739.

9 Weuts, I.; Dycke, F. V.; Voorspoels, J.; Cort, S. D.; Stokbroekx, S.; Leemans, R.; Brewster, M. E.; Xu, D.; Segmuller, B.; Turner, Y. T. A.; Roberts, C. J.; Davies, M. C.; Qi, S.; Craig, D. Q. M.; Reading, M. *J. Pharm. Sci.* **2011**, *100*, 260-274.

10 Jochmans, D.; Anders, M.; Keuleers, I.; Smeulders, L.; Kräusslich H.; Kraus, G.; Müller, B. *Retrovirology* **2010**, *7*, 89-102.

11 ACD/ilab2, version 12.01, Advanced Chemistry Development, Inc., Toronto, ON, Canada, www.acdlabs.com, **2014**.

12 http://www.chemicalize.org/

13 Veber, D. F.; Johnson, S. R.; Cheng, H.; Smith, B. R.; Ward, K. W.; Kopple, K. D. *J. Med. Chem.* **2002**, *45*, 2615-2623.

14 Auwerx, J.; North, T. W.; Preston, B. D.; Klarmann, G. J.; De Clercq, E.; Balzarini, J. *Mol. Pharmacol.* **2002**, *61*, 400-406.

15 Singer, V. L.; Jones, L. J.; Yue, S. T.; Haugland, R. P. *Anal. Biochem.* **1997**, *249*, 228-238.

16 Tucker, T. J.; Saggar, S.; Sisko, J. T.; Tynebor, R. M.; Williams, T. M.; Felock, P. J.; Flynn, J. A.; Lai, M.; Liang, Y.; McGaughey, G.; Liu, M.; Miller, M.; Moyer, G.; Munshi, V.; Perlow-Poehnelt, R.; Prasad, S.; Sanchez, R.; Torrent, M.; Vacca, J. P.; Wan, B.; Yan, Y. *Bioorg. Med. Chem. Lett.* **2008**, *18*, 2959-2966.

17 Pannecouque, C.; Daelemans, D.; De Clercq, E. *Nat. Protoc.* **2008**, *3*, 427-434.

18 Pauwels, R.; Balzarini, J.; Baba, M.; Snoeck, R.; Schols, D.; Herdewijn, P.; Desmyter, J.; De Clercq, E. *J. Virol. Methods* **1988**, *20*, 309-321.

19 Pauwels, R.; Andries, K.; Desmyter, J.; Schols, D.; Kukla, M. J.; Breslin, H. J.; Raeymaeckers, A.; Van Gelder, J.; Woestenborghs, R.; Heykants, J.; Schellekens, K.; Janssen, M. A. C.; De Clercq, E.; Janssen, P. A. J. *Nature* **1990**, *343*, 470-474.

20 Daelemans, D.; Pauwels, R.; De Clercq, E.; Pannecouque, C. *Nat. Protoc.* **2011**, *6*, 925-933.

21 Spitzer, R.; Jain, A. N. *J. Comput. Aided Mol. Des.* **2012**, *26*, 687-699.

22 Jain, A. N. *J. Comput. Aided Mol. Des.* **2007**, *21*, 281-306.

23 Jain, A. N. *J. Med. Chem.* **2003**, *46*, 499-511.

24 Raduner, S.; Majewska, A.; Chen, J. Z.; Xie, X. Q.; Hamon, J.; Faller, B.; Altmann, K. H.; Gertsch, J. *J. Biol. Chem.* **2006**, *281*, 14192-14206.